AD-A118 401 ARMY ARMAMENT RESEARCH AND DEVELOPMENT COMMAND DOVER--ETC F/G 19/1
VISCO-ELASTIC BEHAVIOR OF INCENDIARY COMPOSITIONS UNDER BALLIST--ETC(U)
JUN 82 W H SQUIRE, L W GARNETT

UNCLASSIFIED NL

1 OF 1
AD A
118401

END
DATE FILMED
09-82
DTIC

SQUIRE & GARNETT

18 June 1982

VISCO-ELASTIC BEHAVIOR OF INCENDIARY COMPOSITIONS UNDER BALLISTIC LOADING

WALTER H. SQUIRE
LAMONT W. GARNETT
FIRE CONTROL & SMALL CALIBER WEAPON SYSTEMS LABORATORY
U.S. ARMY ARRADCOM, DOVER, NJ 07801

BACKGROUND

The defeat of both personnel and materiel type targets on the modern battlefield is accomplished in the most cost effective means through the terminal effects of blast, fire, and fragmentation. These terminal effects are quite easily realized through the functioning of a high explosive projectile. While the terminal effects of gun-launched, high explosive projectiles is a well-accepted fact, munition designers must incorporate independent safing, arming, and functioning mechanisms into the munition. In general, gun-launched, high explosive projectiles are required to be safe from accidental or premature initiation during transportation and handling and while being fed into the weapon. However, once the projectile has been launched and directed toward the target, an arming mechanism is required to render -- on a reliable and predictable basis -- the projectile in a state for functioning giver its interaction with the target. Lastly, when the high explosive does engage the target, a functioning mechanism must be provided to initiate the explosive charge in a high order detonation. Traditionally, these performance requirements for independent safing, arming, and functioning are accomplished through a conventional mechanical or electrical fuze. Specific safety requirements for the generic cannon caliber ammunition class of fuzes are provided in reference (1).

Unfortunately, recent tactical trends (i.e. proximity of friendly personnel in the immediate area from which a high explosive projectile has been launched) and a wide diversity of targets on the modern battlefield have driven fuze designers to great lengths in providing for a spectrum of safing, arming, and functioning envelopes in a particular fuze design. A typical cannon caliber projectile fuze (i.e. a fuze which is used on 20 through and including 40mm ammunition) is shown in Figure 1. As is readily seen, safety and performance requirements have dictated a rather complex and sophisticated mechanism. When one considers the relative density of which cannon caliber ammunition is produded on a yearly basis and the cost of a conventional mechanical or electrical fuzing -- resulting from

complexity and sophistication -- the motivation is obvious for simpler and less expensive fuzes.

INTRODUCTION

This motivation for a simpler and less expensive fuze mechanism and yet maintaining the capability to defeat a myriad of targets on a reliable basis has impelled fuze designers to seek novel means of accomplishing the operations of safing, arming, and functioning. One such means which has recently come to the fore is shown in Figure 2. This figure presents a cut-away view of a 20mm, high explosive projectile which does not utilize a conventional mechanical or electrical fuze mechanism. Most of the projectile's attributes/components, however, are of a traditional design. The projectile body, rotating band, external shape, nose cap, high explosive charge, etc., are typical of those employed in other cannon caliber ammunition. Moreover, the assembly of this projectile is effected via standard techniques. The uniqueness of the concept shown in Figure 2 lies in the fact that two different incendiary mechanisms are in the forward (projectile nose) and mid-regions of the projectile. The proposers and advocates of this concept contend that the safing, arming and functioning mechanisms of this concept are accomplished by a physical rearrangement of the forward incendiary mix as a result of ballistic loading. During launch, a 20mm, high-explosive projectile senses a set-back force of approximately 1.2×10^{5} g's and a rotational velocity of 1.7×10^{4} radians/second[2]. Typical in-barrel ballistic times are of the order of $2\text{-}3 \times 10^{-3}$ seconds and the flight time to a target 1000 meters distant is 3-4 seconds. It is within these loading and temporal constraints that the concept shown in Figure 2 must operate.

HYPOTHESIZED SAFING/ARMING/FUNCTIONING MECHANISM

The pre-launch state of the projectile shown in Figure 2 is safe. Since there is no detonator present (by virtue of the fact that there is no conventional fuze present), accidental or premature initiation is impossible. The safety of the projectile is limited only by the safety of the high explosive charge which, unless stimulated by a shock or pressure pulse, is a relatively insensitive material. Without the use of a detonator-type material to generate a pressure wave in the high explosive medium, it is extremely difficult to initiate accidentally the projectile.

PROBLEM STATEMENT

The concept shown in Figure 2 and hypothesized to operate as described in the previous narrative has been demonstrated and evaluated to the point where it may be added to the US's ammunition inventories. For the most part, the concept was matured through a trial-and-error, empirical approach. Given the concept's demonstrated success, it seems reasonable to explore fully all possible design options for fuzing which may attend the rearrangement of an incendiary composition under ballistic loading. For this reason, an analytical model was constructed to predict the movement of an incendiary subject to set-back and centripetal loading. The succinct purpose for formulating the anlaytical model and verifying the model's predictive capability with real-range data is to allow a convenient, rapid

economical means to maximize the safety and performance capabilities of "fuzeless" projectile concept. Once the relationship between the local density of the incendiary and the cavity's formation is known, performance alternatives such as arming delays, delays after impact, super-quick functioning can all be incorporated into the basic design. The analysis which follows will then predict the motion of the locus of points at the interior surface of the projectile's nose under the influence of ballistic loading.

ANALYTICAL APPROACH

The approach pursued in developing the mathematical model is to separate the total event into two phases -- one, the result of set-back or inertial loading and the other attributable to the centripetal loading. The set-back loading will be strongly influenced by the pressure-time history of the propellant gases which cause the projectile's acceleration. The centripetal loading will be a function of the rotational velocity imparted to the projectile as a result of the barrel's rifling. The displacement realized by the forward incendiary due to the set-back loading will serve as the initial condition for the rearrangement due to centripetal loading.

ANALYSIS

The pressure-type history of the propellant gases recorded during the firing of a 20mm cartridge is presented in Figure 4 and is the curve labelled $P^{(2)}$. The curves identified V and T are respectively the projectile velocity and projectile travel. No attempt has been made to convert these data to SI units since they were abstracted directly from (2). The pressure-time curve has been divided into twenty-four time increments, thereby allowing an incremental loading of the projectile. In the first phase of the analysis, the force balance equation is $ma = PA$. The instantaneous set-back force, F_{s_i}, is the product of the projectile mass and the instantaneous acceleration. Figure 5 shows a sketch of the incendiary charge as it is defined by the interior surface of the projectile's nose and the simplification of this geometry to a right circular cylinder. The local stress concentration imparted to the forward face of the incendiary is classically given as

$$\sigma = \frac{F_s}{A_I}$$

Selected values for a, F_{s_i}, and σ as a function of various increments of the pressure-time curve are given below:

$m(\ )$	$P\left(\frac{\text{DYNE}}{\text{CM}^2}\times 10^{-8}\right)$	$a\left(\frac{\text{CM}}{\text{SEC}^2}\times 10^{-7}\right)$	$F_{s_i}\left(\text{DYNE}\times 10^{-7}\right)$	$\sigma\left(\frac{\text{DYNE}}{\text{CM}^2}\times 10^{-7}\right)$
0	0	0	0	0
4	6.9	2.3	4.0	8.8
8	34.5	11.4	20.1	44.2
10	41.4	13.7	24.1	53.0
12	36.6	12.1	21.3	46.9

* All symbols are defined under the NOMENCLATURE heading.

14	24.2	8.0	14.1	31.0
20	9.7	3.2	5.6	12.3
24	6.2	2.0	3.5	4.4

The density profile of the incendiary composition in the projectile's nose is discussed in (3) and is portrayed in Figure 6. A linear approximation to the measured density profile has been effected to facilitate the mathematics. Reference (4) provides background data as to the values of typical densities of incendiary compositions encountered in cannon caliber ammunition. A maximum local density at $\bar{Z}=0$ (i.e. base of the projectile's nose) of 2.95 grams/cc is deduced from reference (4). Hence, the following range of values will be used to describe the local densities in the projectile's nose.

$\rho\left(\frac{GRAM}{cc}\right)$	$\bar{Z}$ (cm)*
2.95	0-7.17
1.62	7.18-16.73
0.29	16.74-23.9

* $\bar{Z}$ is measured from the base of the projectile's nose toward the ogive.

The displacement of the forward surface of incendiary charge will be the result of the compression of the incendiary in each of the three increments ($0\leq\bar{Z}\leq 7.17$, $7.18\leq\bar{Z}\leq 16.73$, $16.74\leq\bar{Z}\leq 23.9$). In general, a material's compressibility is related to the local stress concentration through the Modulus of Elasticity. Classically,

$$\epsilon = \frac{\sigma}{E}$$

In order to calculate the overall displacement of the forward surface, the local stress concentration will be incrementally advanced in time in each of the three regions. Each increment of compression, in turn increases the local density which then requires an updated value for the Modulus of Elasticity. Therefore, for each of the three regions in the incendiary charge, the total compression will be given by:

$$\epsilon_{TOTAL} = \int_0^{t_{FINAL}} \epsilon(t)\,dt = \int_0^{t_{FINAL}} \frac{\sigma(t)}{E}\,dt$$

$$\epsilon_{TOTAL} = \frac{\Delta t}{15}\left[14\left[\frac{1}{2}\left(\frac{\sigma_0}{E_0}+\frac{\sigma_m}{E_m}\right)+\sum_{j=2}^{m-2}\frac{\sigma_j}{E_j}\right]+16\sum_{j=1}^{m-1}\frac{\sigma_j}{E_j}\right] \quad (1)$$

Where each incremental σ_i requires an updated value of the Modulus of Elasticity. For each Δt equation (1) is applied to each of the three regions. The assumption is made that each region realizes the same local stress' concentration for a particular Δt .

Reference (5) provides data on the physical and mechanical properties of solid materials in the density range of 0.29 - 2.95 grams/cc. Porous graphite with a density of 1.02 grams/cc has a Modulus of Elasticity of 1.38 x 10^{10} dyne/cm^2. Local values for E which bracket this value are used as the local density is increased as a result of the compression. The displacement of the forward surface in the rearward direction is the product of the compression and instantaneous length.

The solution of equation (1) and multiplication by the instantaneous length is accomplished via computer and will not be discussed at any greater length. Bookkeeping of the updated values of E is also done within the computer. The range of Modulus of Elasticities assigned to the region adjacent to the ogive varies from 0.46 x 10^{10} to dyne/cm to 0.6[illegible] x 10^{10} dyne/cm^2. Multiplication of the resulting compressions and the instantaneous lengths yields movement of the forward surface by 2.43mm. Also, when equation (1) is applied to elemental discs in the mid and base regions of the incendiary charge where the nominal values of E are 1.86 x 10^{11} dyne/cm^2 and 8.38 x 10^{11} dyne/cm, respectively. The movement of these discs are of the order 10^{-3} and 10^{-4}mm, respectively. The conclusion is reached that the set-back loading perturbs the forward surface of the incendiary charge by displacing it 2.43mm in the rearward direction and that the densities in the mid and base regions of the incendiary are of such magnitude that there is no discernible motion which may be attributable to compression.

Once the initial displacement of the incendiary has been realized and the projectile exists the muzzle of the weapon beginning its free flight, the cavitation prediction is the next step in the analysis. Reference (6) provides a detailed analytical treatment of Couette Flow which involves the steady helical flow of a viscous medium between bounding cylinders rotating with different angular velocities Ω_1, and Ω_2. The analysis undertaken in reference (6) assumes that there is no axial loading. Under the assumption that each material point moves in a circle with speed $r\omega(r)$, the shear stress in the radial direction then becomes

$$S(r) = \frac{M}{2\pi r^2}.$$

Equation (16.11) of reference (6) gives the velocity profile as

$$\omega(r) - \Omega_1 = \int_{R_1}^{r} \frac{1}{\xi} \lambda\left(\frac{M}{2\pi \xi^2}\right) d\xi = \tfrac{1}{2} \int_{\frac{M}{2\pi r^2}}^{\frac{M}{2\pi R_1^2}} \frac{1}{S} \lambda(S)\, dS \qquad (2)$$

where S = shear stress concentration
λ = rate of shear function (an inverse function of S).

As a result of the high shear rates encountered in the spinning of the projectile during its trajectory, non-Newtonian fluids show a characteristic known as ultimate viscosity (second Newtonian viscosity). That is, the non-Newtonian effects are diminished or suppressed at high flow rates (those commensurate with angular velocity of 1.7×10^4 radians/second). This ultimate viscosity simplifies the relationship between the rate of shear function and the shear stress

$$\lambda(s) = \frac{s}{\eta_\infty}.$$

Substitution of the above expression into equation (2) and evaluation yields

$$\omega(r) = \frac{1}{R_2 - R_1}\left[r\left(\Omega_2 R_2^2 - \Omega_1 R_1^2\right) - \frac{R_1^2 R_2^2}{r}\left(\Omega_2 - \Omega_1\right)\right] \tag{3}$$

which is consistent with the classical Couette Flow problem solution. In order to predict the cavitation in the viscous medium, reference (6) is again used as the basis. Coleman, *et al* [6] provide the governing equation for the climbing effect in Couette Flow as equation (20.1)

$$\gamma = \int_{R_1}^{r}\left\{\frac{1}{\xi}\left[\sigma_2\left(\frac{M}{2\pi\xi^2}\right) - \sigma_1\left(\frac{M}{2\pi\xi^2}\right)\right] - \rho\{\omega(\xi)^2\}\right\} d\xi - \sigma_1\left(\frac{M}{2\pi r^2}\right) + q(t) \tag{4}$$

where γ = total normal stress in the axial direction
ξ = variable of integration

$q(t)$ is determined from the balance of the total force in the axial direction

$$2\pi \int_{R_1}^{R_2} \gamma r\, dr = -r_0 \pi \left(R_2^2 - R_1^2\right). \tag{5}$$

STAMP Security Classification here

Substitution of equations (4) and (5) into (3) and rearranging gives

$$p = -p_0 + \frac{1}{R_2^2 - R_1^2} \int_{R_1}^{R_2} \left\{ \rho (R_2^2 - R_1^2) r \omega(r)^2 - \frac{R_2^2 - r^2}{r} \sigma \left(\frac{M}{2\pi r^2} \right) + \frac{R_2^2 + r^2}{r} \sigma \left(\frac{M}{2\pi r^2} \right) \right\} dr. \tag{6}$$

Denoting X as the excess of the atmospheric pressure p_0 over the thrust $-T$ exerted by the fluid in the axial direction

$$X = p_0 + T.$$

In general, X is not zero and hence the face surface at the upper end of the fluid mass cannot be a plane Z = constant. The derivative of X in the radial direction is obtained from equation (6)

$$\frac{\partial X}{\partial r} = -\rho r \omega(r)^2 + \frac{1}{r} \left[\sigma_2 \left(\frac{M}{2\pi r^2} \right) - \sigma_1 \left(\frac{M}{2\pi r^2} \right) \right] + \frac{M}{\pi r^3} \sigma_1 \left(\frac{M}{2\pi r^2} \right).$$

In the above equation Ω_1 and R_1 were driven to zero to allow the Couette Flow to approximate the centripetal loading of the projectile.

If the normal stress functions are zero, then

$$\frac{\partial X}{\partial r} = -\rho r \omega(r)^2 < 0. \tag{7}$$

This inequality is regarded as an indication that the free surface will slope upwards from the inner to the outer cylinder. Solution of equation (7) and subsequent plotting is the cavitation profile. Figure 7 shows the calculated dependence of $\omega(r)$ on r which is used to calculate the cavitation profile shown in Figure 8.

EXPERIMENT

Recently, an experimental endeavor was undertaken to verify the existence of the cavitation in the forward incendiary composition. An array of X-ray tubes was positioned approximately 200 meters from the muzzle of the weapon in a position which was directly aligned with the projectile's flight path. The tubes were pulsed when the projectile interacted with a break circuit positioned immediately before the "vision" cone of the X-ray tubes. Due to differences in the material thicknesses of various portions of the projectile's body -- the nose is relatively thin, whereas the projectile body is rather thick -- it is impossible to view the entire contents of the projectile. For this reason, the exposure and power levels of the X-ray tubes were adjusted to view only the nose region. Figure 9 is a reproduction of a typical X-ray. Note the cavity shown in Figure 9 is very similar to that predicted from equation (7) and graphed in Figure 8.

CONCLUSIONS

1. Set-back forces are of sufficient magnitude to cause a rearward displacement of the forward surface of the incendiary by 2.43mm.
2. Centripetal forces are responsible for a cavity's formation. The shape of which may be predicted by equation (7) and graphed in Fig. 8.
3. The hypothesized safing and arming mechanism of the "fuzeless" concept has been verified.
4. The analysis described herein offers a design tool -- to maximize the effectiveness of the fuzeless concept particularly relative to definition of the local density.

REFERENCES

(1) MIL-STD-1316B, Military Standard, Fuze Design, Safety Criteria for, 15 February 1977.

(2) Corner, J., Theory of Interior Ballistics of Guns, N.Y., N.Y., John Wiley & Sons, Inc., 1950.

(3) Design Parameters and Functioning Mechanisms, The Multipurpose Concept for Multiple Effects Projectiles, Volume 2, A/S Raufoss Ammunisjonsfabrikker, Raufoss, Norway, December 1964.

(4) AMC Pamphlet 706-177, Engineer Design Handbook, Explosive Series, Properties of Explosives of Military Interest, 1964.

(5) Perry, Robert H. and Chilton, Cecil H., Chemical Engineer's Handbook, Fifth Edition, 1974.

(6) Coleman, B. D., Markovitz, H., Noll, W., Viscometric Flows of Non-Newtonian Fluids, Springer-Verlag New York, Inc., N.Y., N.Y., 1966.

NOMENCLATURE

Symbols are listed in the order in which they are used in the paper.

- P = Instantaneous Chamber Pressure
- T = Projectile Travel
- V = Projectile Velocity
- m = Projectile Mass
- a = Instantaneous Acceleration
- A_p = Bore Area
- F_{SB} = Instantaneous Set-Back Force
- σ = Local Stress
- A_H = Effective Cross-Sectional Area of Incendiary Charge
- N = Increment Number
- ρ = Density
- z = Axial Distance
- ϵ = Compression
- E = Modulus of Elasticity
- t = Time
- i = Summation Index
- t_{exit} = Time to Projectile Exit from Muzzle
- Ω_1 = Applied Angular Velocity
- Ω_2 = Applied Angular Velocity
- u = Displacement in Radial Direction
- τ = Shear Stress
- M = Torque
- ω = Angular Velocity (as a function of radial distance)
- η_0 = Ultimate Viscosity
- $\dot{\gamma}$ = Rate of Shear Function
- ξ = Variable of Integration
- σ_z = Total Normal Stress in Axial Direction
- q = Excess Atmospheric Pressure over Thrust
- P_o = Atmospheric Pressure

FIGURES

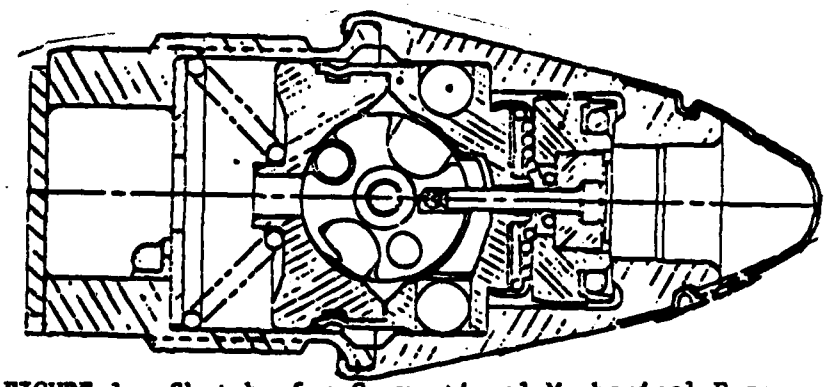

FIGURE 1. Sketch of a Conventional Mechanical Fuze

STAMP Security Classification here

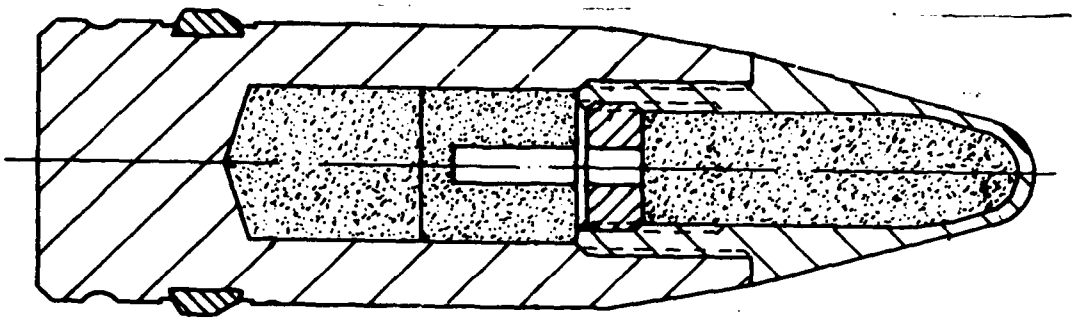

FIGURE 2. Novel High Explosive Projectile

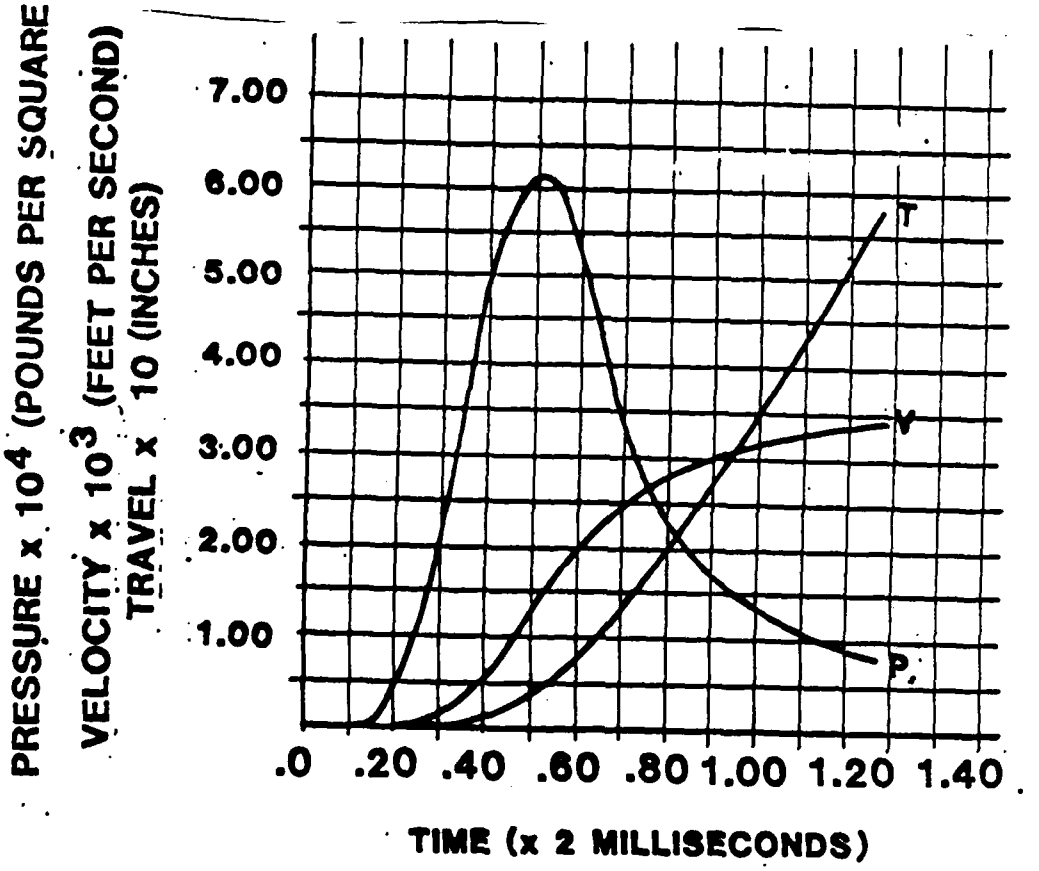

FIGURE 4. Pertinent 20mm Interior Ballistic Data

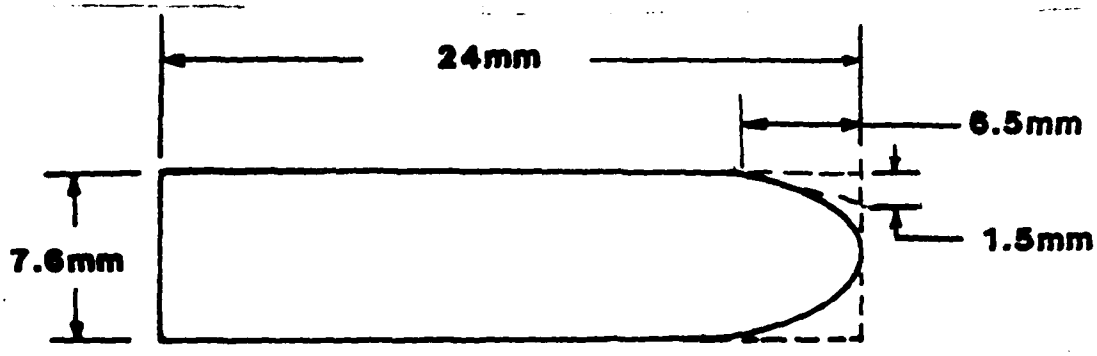

BODY 1-INCENDIARY CHARGE (B)

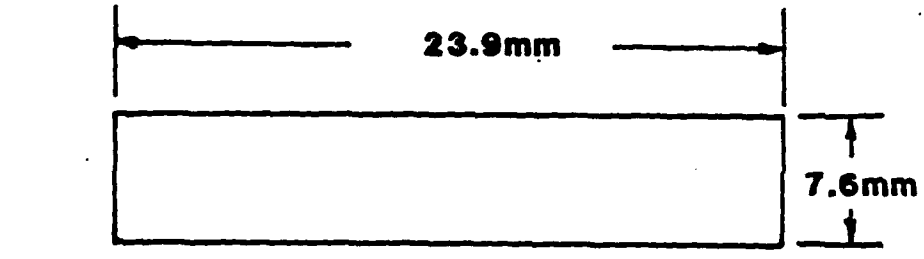

RIGHT CIRCULAR CYLINDER MODEL

FIGURE 5. Dimensions and Simplifications of Forward Incendiary

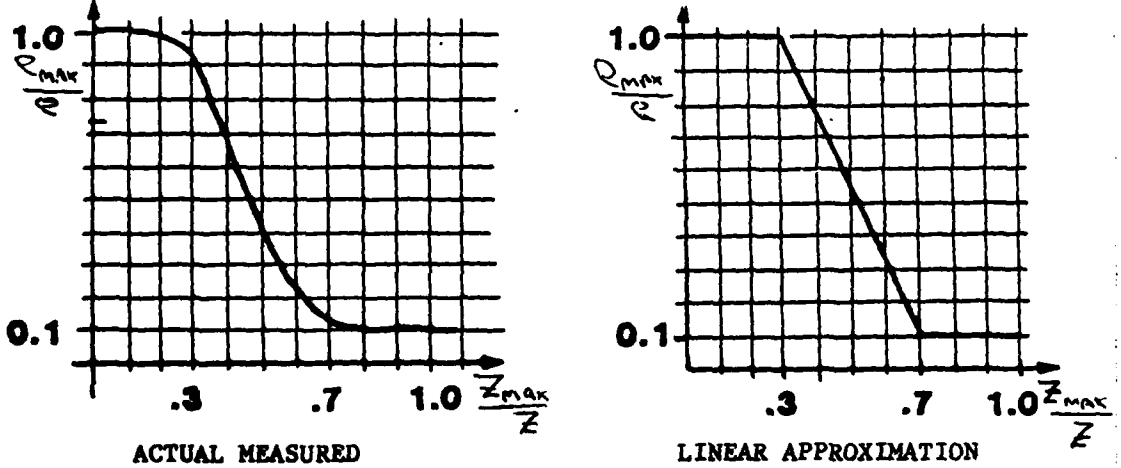

ACTUAL MEASURED

LINEAR APPROXIMATION

FIGURE 6. Density Profile and Approximation in Forward Incendiary Charge

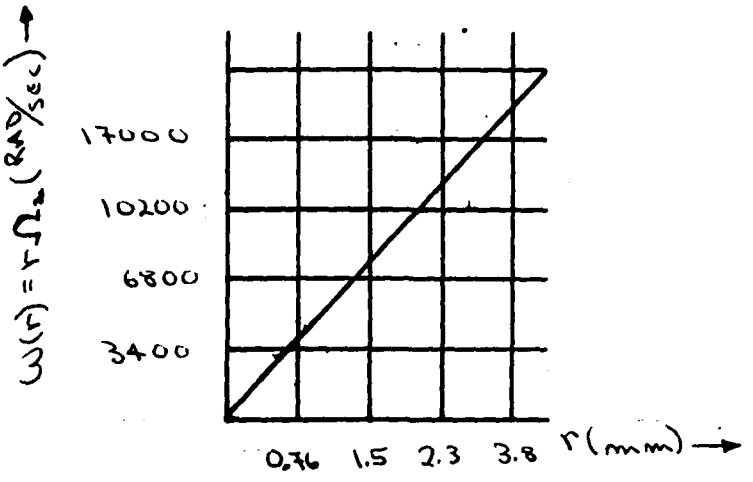

FIGURE 7. Plot of $\omega(r)$ Versus r Used to Evaluate Equation (7).

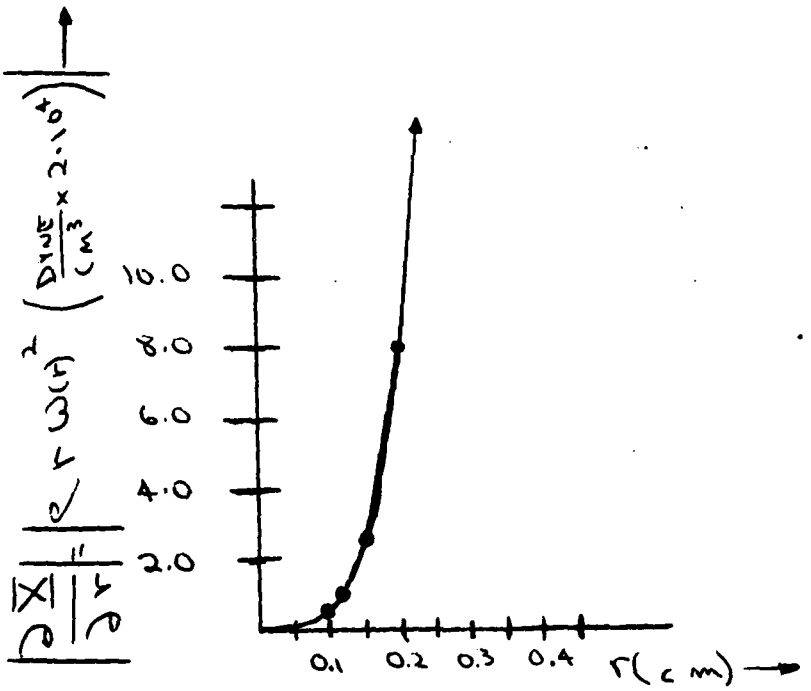

FIGURE 8. Plot of Equation (7) Showing Parabolic Shape of Cavity.

FIGURE 9. Dynamic X-ray of Forward Incendiary Showing Cavitation


FILMED
9-8